The 3rd International Innovation Technology Proceedings
Vol 3 No 1 (2025): October
E-ISSN: 3030-9948
https://iite-proceeding.poltekindonusa.ac.id

Influence of Sprue Layout on Microstructure, Porosity, And Mechanical Properties of Aluminum Pipe Casting with Red Sand Molding Write

Wibi Pramanda[1*], Maulana Singgih Pratama[2], Mazwan[3]
[1,] Heavy Equipment Maintenance Engineering Technology, Jambi Polytechnic
[2] Mechanical Engineering, Muhammadiyah University of Surakarta
[3] Mechanical Engineering, Jambi Polytechnic
*Corresponding author email: wibi@politeknikjambi.ac.id

Received:	Revised:	Accepted:	Published:
July 22, 2025	July 29, 2025	July 31, 2025	October 31, 2025

Abstract

This study investigates the effect of sprue position on the characteristics of recycled aluminum castings, focusing on chemical composition, microstructure, porosity, and hardness. Recycled aluminum from various remelted components was used to promote sustainability in metal casting. Three sprue configurations were tested—top (A), side (B), and center (C). The analysis included chemical composition (ASTM E-1251), microstructure via metallographic microscopy (ASTM E-3), porosity observation, and Brinell hardness testing (ASTM E-10). The results showed a composition of 81.20% aluminum, 11.80% silicon, and 4.50% iron, classifying the material as an Al–Si alloy. The sprue position significantly influenced casting quality. Sprue A achieved the highest hardness value (99.48 BHN) and the finest microstructure with minimal porosity. In contrast, positions B and C had lower hardness values (79.04 BHN and 74.11 BHN, respectively) and coarser microstructures, due to increased porosity. This study highlights the importance of sprue design in minimizing casting defects and improving the mechanical performance of recycled aluminum alloys.

Key words: *Sprue Position, Al-Si Alloy, Porosity Defects, Brinell Hardness, Microstructure Analysis*

1. Introduction

Metal casting is one of the oldest manufacturing processes that remains relevant for producing machine components with complex shapes. Materials such as aluminum are widely used in various industrial and construction applications due to their lightweight nature, corrosion resistance, and good strength when combined with other elements [1]. In the casting process, the quality of the final product is greatly influenced by the gating system used, which plays a crucial

role in directing molten metal into the mold [2]. Various casting defects, such as porosity and shrinkage, often occur and can reduce the mechanical properties of the product, including its hardness. Therefore, optimal casting methods continue to be developed to minimize defects and improve product quality [3].

Various studies on metal casting have been conducted, focusing on factors such as the shape of the sprue, the riser design, and the location of the in-gate to reduce porosity defects and improve the hardness and grain structure of aluminum alloys [4]. However, research that specifically compares variations in sprue position (top, side, and center) on pipe products using red sand molds remains limited. A deeper understanding of how sprue positioning affects pouring rate, defect formation, and the mechanical properties of the product still needs to be explored [5].

This study proposes an approach to directly analyze the influence of three different sprue positions—top, side, and center—on the outcome of aluminum castings. The approach aims to identify the most effective sprue configuration for minimizing porosity defects, which in turn enhances hardness values and produces finer microstructures [6]. The results of this study are expected to provide practical guidance for the casting industry in selecting the optimal sprue position for pipe casting products using red sand molds.

The objective of this study is to comprehensively analyze the influence of different sprue positions on the chemical composition, porosity defects, hardness, and microstructure of aluminum pipe casting products. [7][8]. Brinell The methods to be used include chemical composition testing, microphotography analysis, porosity defect observation, and Brinell hardness testing [9].

2. Method

Specimen This study adopts an experimental approach to investigate the effect of sprue position variations on the quality of aluminum castings in pipe products. The methodology is divided into three main stages: material preparation, casting process, and specimen characterization.

2.1 Material Preparation and Methods

The raw material used is recycled aluminum or scrap sourced from various origins. To create the mold, this study utilizes red sand molds, which are a mixture of sand, clay as a binder, and

water [10]. The main equipment utilized includes a melting furnace, a thermocouple for temperature monitoring, and various instruments for material testing.

2.2 Melting and Casting Process

Aluminum is melted in a furnace at a melting temperature of approximately 750°C. Once the molten metal is ready, the pouring process is carried out into the sand mold [11]. In this study, three different sprue configurations—top, side, and center—are applied to investigate their impact on the quality of aluminum pipe castings:

1. Position A (Top): Molten metal is poured from the top of the mold, resulting in a fast and direct flow into the mold cavity without the need for an additional in-gate.
2. Position B (Side): Pouring is done from the side, with the metal flowing through an in-gate before filling the mold cavity.
3. Position C (Center): The sprue is placed at the center of the mold, producing a slower and longer flow, which may potentially affect the solidification process.

After pouring, the casting is allowed to cool and solidify, after which the product is removed and cleaned of any remaining mold residues [12].

2.3 Specimen Preparation and Testing

Test specimens are prepared from the finished casting products and tested according to relevant technical standards:

1. Chemical Composition Test: The analysis of elemental content in the casting material is conducted using a spectrometer, based on the ASTM E-1251 [13].
2. Brinell Hardness Test: The material hardness is measured using a Brinell hardness testing machine with a load of 500 Kgf and a 10 mm diameter ball indenter, in accordance with ASTM E-10 [14].
3. Porosity Defect Observation: Samples are examined both visually and quantitatively to detect the presence of air voids formed during the solidification process.
4. Microstructure Test (Microphotography): Specimens are prepared for microstructural observation using a metallographic microscope at magnifications of 100x, 200x, and 500x,

following the ASTM E-3 standard [15]. This test aims to identify the morphology of aluminum and silicon crystal grains [16].

3. Result and Discussion

"This section presents the results of a series of tests conducted on aluminum casting products with varying sprue positions, followed by an in-depth analysis and discussion of the findings.

3.1 Chemical Composition Test Results

Based on chemical composition testing conducted using a spectrometer, the casting material was identified as an aluminum-silicon (Al-Si) alloy. The average composition showed an aluminum (Al) content of 81.20% and a silicon (Si) content of 11.8%. Additionally, other elements were detected, such as iron (Fe) at 4.50%. The composition of the test samples can be seen in Table 1. The relatively high silicon content positively affects casting characteristics, such as facilitating the pouring process, reducing shrinkage, and enhancing corrosion resistance. However, excessive silicon levels may reduce the material's ductility. The iron (Fe) content of 4.50% serves to prevent molten metal from sticking to the mold, but an overly high concentration can degrade mechanical properties, including tensile strength, and increase the risk of porosity defects

Table 1. Chemical Composition of Aluminum Casting

Element	Test Specimen (%)	Standard Deviation
Al	81,20	3,214
Si	11,8	2,11
Fe	4,50	0,382
Cu	0,0906	0,0206
Mn	0,130	0,0974
Mg	0,115	0,113
Cr	0,117	0,124
Ni	0,0133	0,196
Zn	0,270	0,353
Sn	0,0953	0,0524

3.2 Brinell Hardness Test Results

The Brinell hardness test revealed significant variation among the three sprue positions. The highest hardness value was found in the specimen with sprue position A, measuring 99.48 BHN. The hardness value for sprue position B was recorded at 79.04 BHN. The lowest value was observed in the specimen with sprue position C, at 74.11 BHN. The specimens can be seen in Figure 1, while a summary of the Brinell hardness test results is presented in Table 2.

Fig. 1. Sprue Specimens

The highest hardness value observed in sprue position A can be attributed to the faster flow rate of the molten metal. This rapid pouring rate is effective in minimizing the formation of porosity defects and results in a finer grain structure. In contrast, sprue position C, with its slower flow rate, allows for more porosity defects to form, which significantly reduces the hardness value

Table 2. Brinell Hardness Test

No	Sprue Position	Brinell Hardness (HB) Values					Average HB
1	Top	100.41	100.21	99.88	99.70	99.34	99.48
2	Side	79.56	79.20	76.75	76.68	79.47	79.04
3	Center	74.10	73.59	74.03	73.99	73.95	74.11

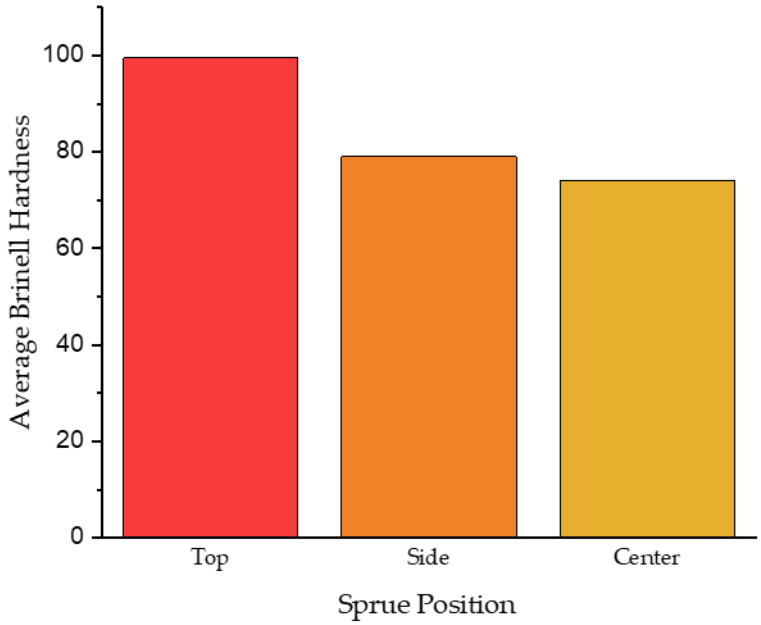

Fig. 2. Average Brinell Hardness Value

3.3 Porosity Defect Observation

Visual and microscopic observations revealed a strong correlation between sprue position and the level of porosity defects. Specimens cast using sprue position C exhibited the highest porosity, followed by position B, while the lowest porosity was observed in position A. The high porosity in sprue position C is attributed to the slower flow rate of molten metal, which allows partial solidification before the mold cavity is fully filled, thereby trapping gas. In contrast, sprue position A enables a faster and more direct flow, minimizing the likelihood of gas entrapment and resulting in significantly lower porosity. Observations were conducted using an optical microscope, and specimen images were processed using the ImageJ application to enhance the visual representation of porosity [17].

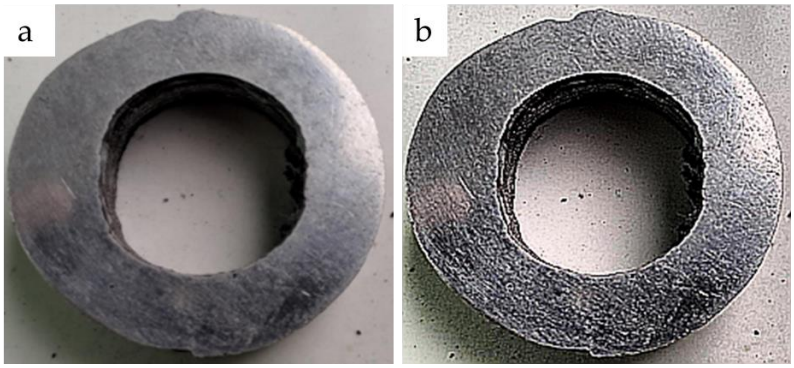

Fig. 3. Specimen Appearance at Top Sprue Position (A): (a) Before Processing, and (b) After Processed Using ImageJ Application

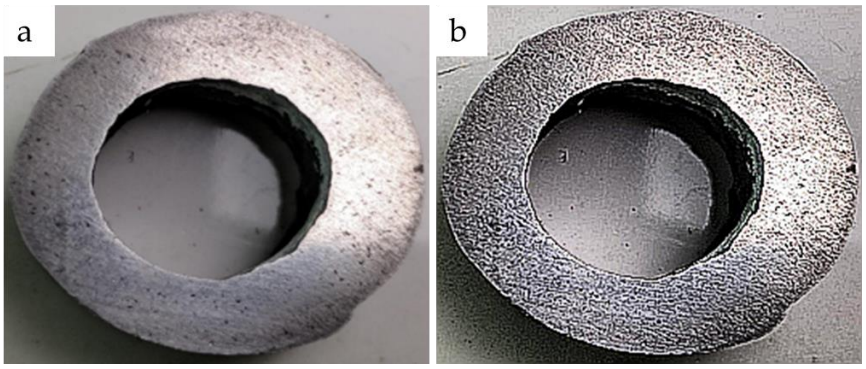

Fig. 4. Visual representation of the specimen cast with side sprue position (B): (a) unprocessed image, and (b) enhanced image following analysis using ImageJ software to highlight porosity features

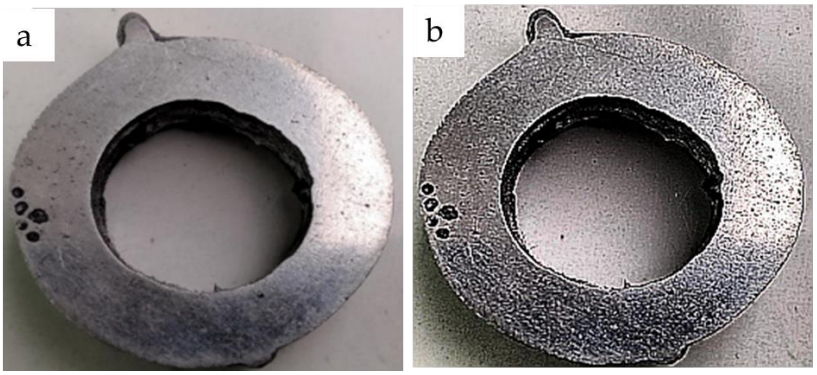

Fig. 5. Visual representation of the specimen cast with center sprue position (C): (a) unprocessed image, and (b) enhanced image following analysis using ImageJ software to highlight porosity features.

3.4 Microstructure Analysis

Microstructural observations using a metallographic microscope at 500x magnification revealed that the specimen structure consists of two primary phases: large, white aluminum (Al) grains and fine, elongated silicon (Si) particles resembling needles. A direct correlation was observed between hardness values and grain size. The specimen with the highest hardness, cast using sprue position A, exhibited the finest (smallest) crystal grains. In contrast, specimens from sprue positions B and C, which showed lower hardness values, tended to have larger crystal grains. This confirms that an optimal pouring rate can produce a more homogeneous and refined microstructure, contributing to improved mechanical properties of the material

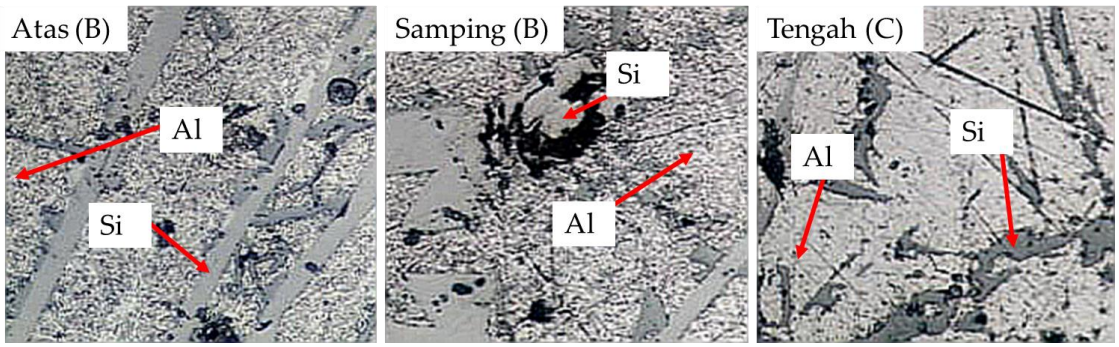

Fig. 6. Microscopic View of Specimens at 500x Magnification for Each Sprue Position: A (Top), B (Side), and C (Center)

4. Conclusion

Based on the analysis of the research findings, several key points can be concluded regarding the influence of sprue position in the aluminum casting process:

1. Influence of Sprue Position on Casting Quality: This study demonstrates that the placement of the sprue is a significant factor affecting the quality of the casting product. The top sprue position (A) resulted in the highest casting quality, while the center sprue position (C) produced the lowest
2. Relationship Between Hardness, Porosity, and Flow Rate: An inverse relationship was found between material hardness and porosity level. A faster pouring rate, as observed in the top sprue position (A), proved effective in reducing porosity defects, which directly

increased the material's hardness to the highest value of 99.48 BHN. Conversely, the slower flow rate in the center sprue position (C) led to greater porosity formation, resulting in a significant decrease in hardness to 74.11 BHN.

3. Influence of Flow Rate on Microstructure: The pouring rate affects not only macro-level defects but also plays a crucial role in the formation of the material's microstructure. The top sprue position (A), which exhibited the highest hardness, produced the finest crystal grains. This indicates that a fast and uniform flow promotes a more consistent solidification process, resulting in a more homogeneous microstructure and contributing to enhanced mechanical properties.

5. References

[1] C. Ji, X. Di, X. Liu, S. Liu, J. Song, and H. Huang, "Multi-field coupling analysis of twin-roll casting process for achieving thin aluminum strip high-speed casting and fabricating laminated metal cladding materials," *Case Stud. Therm. Eng.*, vol. 72, no. November 2024, 2025, doi: 10.1016/j.csite.2025.106423.

[2] B. Z. R. Lee, L. He, S. S. Chong, and H. Li, "Mechanical properties of the GS24Mn4 steel - Inconel 718 interface manufactured by laser metal deposition and compound casting," *Mater. Charact.*, vol. 225, no. April, p. 115102, 2025, doi: 10.1016/j.matchar.2025.115102.

[3] S. Namchanthra *et al.*, "Numerical analysis of molten iron flow and heat transfer in plumbing casting defect detection using split tracking approach," *Case Stud. Therm. Eng.*, vol. 72, no. May, p. 106287, 2025, doi: 10.1016/j.csite.2025.106287.

[4] S. R. Sama, T. Badamo, P. Lynch, and G. Manogharan, "Novel sprue designs in metal casting via 3D sand-printing," *Addit. Manuf.*, vol. 25, no. November 2018, pp. 563–578, 2019, doi: 10.1016/j.addma.2018.12.009.

[5] F. Li, Z. Yang, J. Guo, Z. Li, Z. Ma, and L. Bai, "Simulation and optimization of the casting process for a new commercial," *J. Mater. Res. Technol.*, vol. 38, no. July, pp. 1355–1366, 2025, doi: 10.1016/j.jmrt.2025.08.008.

[6] Y. Xu, G. Li, W. Jiang, J. Zhan, Y. Yu, and Z. Fan, "Investigation on characteristic and formation mechanism of porosity defects of Al–Li alloys prepared by sand casting," *J. Mater. Res. Technol.*, vol. 19, pp. 4063–4075, 2022, doi: 10.1016/j.jmrt.2022.06.148.

[7] P. Ferro, A. Fabrizi, F. Bonollo, and F. Berto, "Influence of aluminum casting alloys chemical composition on the interaction with a 304L stainless steel insert," *Procedia Struct. Integr.*, vol. 33, no. C, pp. 189–197, 2021, doi: 10.1016/j.prostr.2021.10.023.

[8] G. Cempura, R. Cygan, and A. Grabo, "Microstructure and resultant properties of ex-situ Alloy 625 + TiB 2 nanocomposites processed via suction casting as filler material for Ni-based superalloys repair applications," vol. 38, no. June, pp. 2820–2839, 2025, doi: 10.1016/j.jmrt.2025.08.032.

[9] I. G. Akande, A. O. Taiwo, and O. S. I. Fayomi, "Surface and corrosion properties of corn cob and egg shell particles reinforced AA3104-H19 composite via stir casting process," *Hybrid Adv.*, vol. 3, no. June, p. 100061, 2023, doi: 10.1016/j.hybadv.2023.100061.

[10] G. P. Borikar and S. T. Chavan, "Optimization of Casting Yield in Multi-cavity Sand Moulds of Al-alloy Components," *Mater. Today Proc.*, vol. 28, no. xxxx, pp. 819–824, 2019, doi: 10.1016/j.matpr.2019.12.305.

[11] S. Lubis and I. Siregar, "Proses Pengecoran Aluminium Sebagai Bahan Pembuatan Blok Silinder," *J. MESIL (Mesin Elektro Sipil)*, vol. 1, no. 1, pp. 30–37, 2020, doi: 10.53695/jm.v1i1.14.

[12] S. B. Gopalkrishna, G. A. Kulkarni, S. Ryll, and E. Specht, "Heat transfer analysis during quenching of moving metal plates using water jets from a mold," *Therm. Sci. Eng. Prog.*, vol. 64, no. June, p. 103792, 2025, doi: 10.1016/j.tsep.2025.103792.

[13] M. D. Vijayakumar, V. Dhinakaran, T. Sathish, G. Muthu, and P. M. B. Ram, "Experimental study of chemical composition of aluminium alloys," *Mater. Today Proc.*, vol. 37, no. Part 2, pp. 1790–1793, 2020, doi: 10.1016/j.matpr.2020.07.391.

[14] F. Taruyun Hudeardo Sinaga, E. Putra Dairi Boangmanalu, J. Fan HT Saragi, and A. Bahri Pratama, "Analisis Sifat Mekanik Material Plat Baja ST 37 Dengan Metode Brinell Hardness Test," *Atech-i*, vol. 1, no. 2, pp. 1–8, 2024, doi: 10.55043/atech-i.v1i2.19.

[15] E. Febriyanti, A. Fadli, A. Suhadi, R. Riastuti, B. Besar, and T. Kekuatanstruktur, "PERUBAHAN MORFOLOGI STRUKTUR MIKRO PADUAN Cu-Zn 70/30 YANG DILAKUKAN TMCP DI SUHU 300°C," *Sintek J.*, vol. 12, no. 1, pp. 1–8, 2018, [Online]. Available: http://jurnal.umj.ac.id/index.php/sintek

[16] E. Sundari, "Rancang bangun dapur peleburan alumunium bahan bakar gas," vol. 3, no. April, 2011.

[17] I. M. Ibrahim, G. Will, X. Wang, R. Clegg, and S. Bell, "Development of a novel deleterious phases analysis and detection method for stainless steel," *Mater. Charact.*, vol. 228, no. June, p. 115363, 2025, doi: 10.1016/j.matchar.2025.115363.

[18] M. R. Braun, P. Walton, S. B. M. Beck, and W. London, "Illustrating the relationship between the coefficient of performance and the coefficient of system performance by means of an R404 supermarket refrigeration system," *Int. J. Refrig.*, vol. 70, pp. 225–234, 2016, doi: 10.1016/j.ijrefrig.2015.10.020.

[19] Z. Ma, H. Bao, and A. P. Roskilly, "Thermodynamic modelling and parameter determination of ejector for ejection refrigeration systems," *Int. J. Refrig.*, vol. 75, pp. 117–128, 2017, doi: 10.1016/j.ijrefrig.2016.12.005.